Journal of Microscopy, Vol. 214, Pt 1 April 2004, pp. 27–35
Received 10 April 2003; accepted 23 October 2003

Shape control of near-field probes using dynamic meniscus etching

L. H. HABER, R. D. SCHALLER, J. C. JOHNSON &
R. J. SAYKALLY
Department of Chemistry, University of California, Berkeley, CA 94720–1460, U.S.A.

Key words. Compound parabolic concentrator, etching techniques, meniscus formation, near-field optics, NSOM, optical fibre probes, scanning microscopy, throughput efficiency, tip cone angle, tip shape.

Summary

Dynamic etching methods for fabricating fibre optic tips are explored and modelled. By vertically translating the fibre during etching by an HF solution under an organic protective layer, a variety of tip shapes were created. The probe taper lengths, cone angles and geometrical probe shapes were measured in order to evaluate the dynamic meniscus etching process. Fibre motion, etching rate, meniscus distortion and etching time were all found to be important variables that can be used to control the final probe shape.

Introduction

Near-field scanning optical microscopy (NSOM) is a powerful tool for subwavelength-resolution spectroscopy and imaging. The subwavelength optical spatial resolution of NSOM is determined largely by the diameter of the fibre probe tip (Paesler & Moyer, 1996; Ohtsu, 1998; Dunn, 1999), as well as the tip–sample distance. The optical throughput is determined by the tip diameter and by the distance over which the evanescent field must traverse until it can propagate. Hence, the size and shape of an NSOM probe should be optimized for a particular application.

Many publications discuss methods for fabricating NSOM tips. The two most common techniques are adiabatic pulling and chemical etching. The pulling technique has been quite well characterized (Valaskovic *et al.*, 1995; Liu *et al.*, 1998) and generally results in tips with small cone angles, which yield low optical throughput but high spatial resolution. There are two different general etching techniques, meniscus etching and selective etching. The latter has been pioneered primarily by Ohtsu and involves the use of variable concentrations of HF, NH_4F and BHF to etch single-mode and multimode fibres into selected tip geometries (Ohtsu, 1998).

Correspondence to: Dr Richard Saykally. Fax: +1 510 6428566; e-mail: saykally@uclink4.berkeley.edu

Meniscus etching employs an organic protective solvent that forms a layer above the acid. The meniscus formed at the liquid–liquid and liquid–solid interfaces changes height as a function of the fibre radius. The etching of SiO_2 fibres by HF is an isotropic etching process (Unger *et al.*, 1998) so the fibre is a cylinder of decreasing radius below the meniscus. At the meniscus, the decreasing radius causes the meniscus height to drop steadily, resulting in a conical tip shape. Different organic layers produce different cone angles (Hoffman *et al.*, 1995; Sayah *et al.*, 1998) ranging from 8.5 to 41°.

Other techniques have been used in conjunction with meniscus etching for greater control of the tip shape. The fibre can be submersed in HF after it has formed a cone to increase the angle of the tip (Jia-Lin *et al.*, 2001). The fibre can be positioned just barely to touch the acid and then etched again to make a double taper (Chuang *et al.*, 1998). The etching process can be combined with pulling (Islam *et al.*, 1997). The fibre can be etched through the cladding to make smoother tips (Lambelet *et al.*, 1998; Stöckle *et al.*, 1999). The tip can also be bevelled by motorized grinding on an aluminium plate to improve and smoothen the shape (Held *et al.*, 2000). Focused ion beam (FIB) fabrication (Spajer *et al.*, 2000; Krogmeier & Dunn, 2001) of fibre probes has also been shown to be a powerful tool for highly controlled tip production, although the high cost is prohibitive.

A recently demonstrated technique for probe fabrication is the dynamic etching method, in which the fibre is translated vertically while being etched (Muramatsu *et al.*, 1999). By moving the fibre at variable speeds for different times, a variety of tip shapes can be created. In the following, we show that dynamic etching results in good control over the probe taper length, cone angle and probe geometry.

Five different types of dynamic meniscus etching techniques are employed in this study: stepped fibre motion, constant fibre speed (Type 1, 2 and 3; explained below) and accelerating fibre motion. Whereas the former method is performed to determine the etching rate for the studied fibre and to ascertain

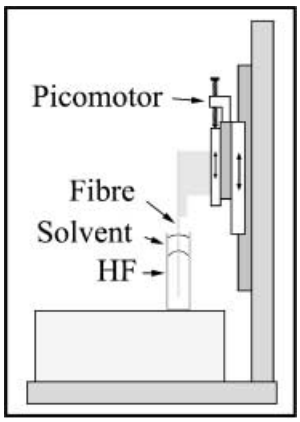

Fig. 1. Dynamic meniscus etching experimental set-up.

whether the etching process is isotropic, the constant fibre speed and accelerating fibre motions can be used to control the probe properties.

Experimental

Figure 1 shows the experimental dynamic meniscus etching set-up. The fibre was positioned in the centre of the tube that contained the two-phase etching solution. Two translation stages controlled the fibre's vertical position; one allowed for gross fibre positioning and the other provided fine motion via a motorized micrometer (Newfocus, Picomotor). To minimize external vibrations of the fibre and etching solution, the etching platform was placed on a lead brick and a large plexiglas box was placed over the entire set-up.

Fibres (3M single mode, 125 μm core, 650 nm) were etched with 49% aqueous HF with an organic protective layer of 1-bromodecane. Prior to etching, the fibre end to be etched was soaked in acetone for 7 min to remove the acrylate jacket. The direction, speed and time of the fibre motion were controlled by computer. After each tip was etched, the fibre was pulled out of the etching solution at 1224 μm min^{-1} for 1–5 min then raised further using the coarse translation stage. Scanning electron microscopy (SEM) was used to characterize (following evaporative deposition of a 50-nm-thick gold coating) tip shapes, lengths and angles. With each of the etching techniques used here, tip diameters of ~20–100 nm were achieved.

Results and discussion

The stepped fibre motion technique principally holds a fibre still throughout the etching process, but at certain time intervals, the fibre is quickly raised (at 1224 μm min^{-1}) by 50–200 μm, creating a 'step'. This technique resulted in tip shapes similar to those shown in Fig. 2, made of the conical tapers from the stationary etching, and cylindrical sections from the steps. The lengths of the cylinders are determined by the distance that the fibre moves, and the radii are determined by the time

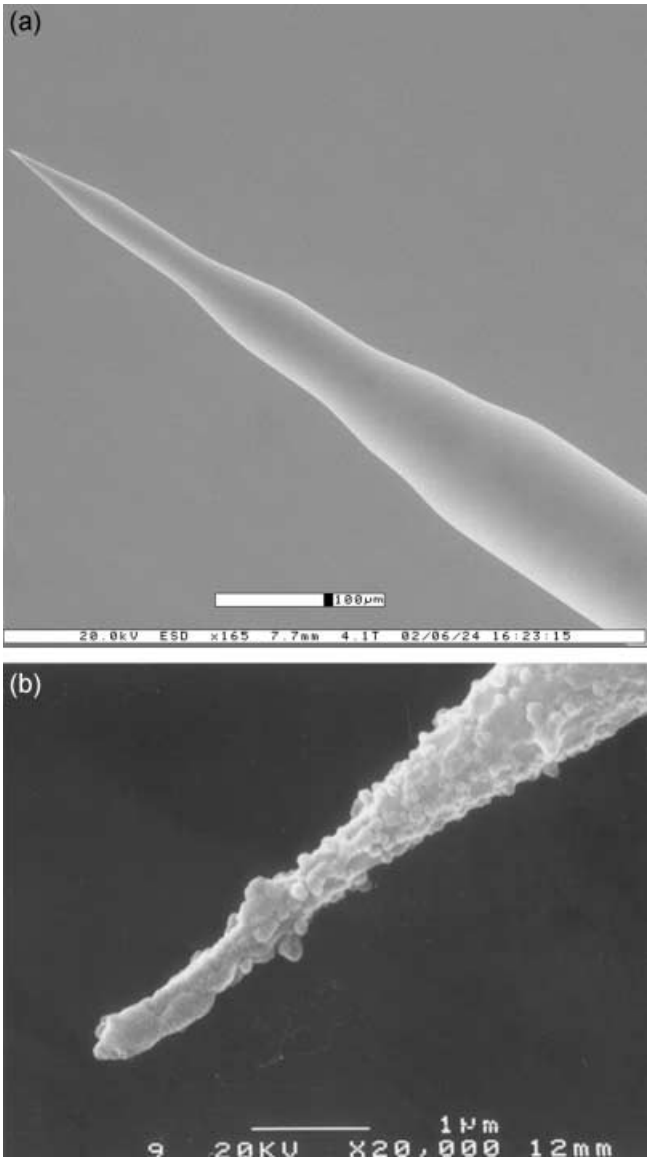

Fig. 2. (a) SEM image of a stepped tip (scale bar = 100 μm). (b) SEM image of another stepped tip (scale bar = 1 μm) with a very thin cylinder of diameter ~520 nm, showing that the cylinder radius can be made quite small. Bumps on the tip are caused by gold particles.

at which the steps were made. Earlier steps have larger radii than later steps.

The formation of the stepped probe shape is due to the isotropic (Unger *et al.*, 1998) nature of the etching process. After the fibre is raised, the fibre is kept stationary again and another conical taper begins where the meniscus touches the raised cylindrical step. Many different steps can be made at different times during the etching process until the cylinder under the meniscus is completely etched away (Fig. 3a,b). The radius of each cylindrical step is the radius of the fibre under the meniscus at the time each step is made, thus measuring fibre radius as a function of time. Six different stepped tips were

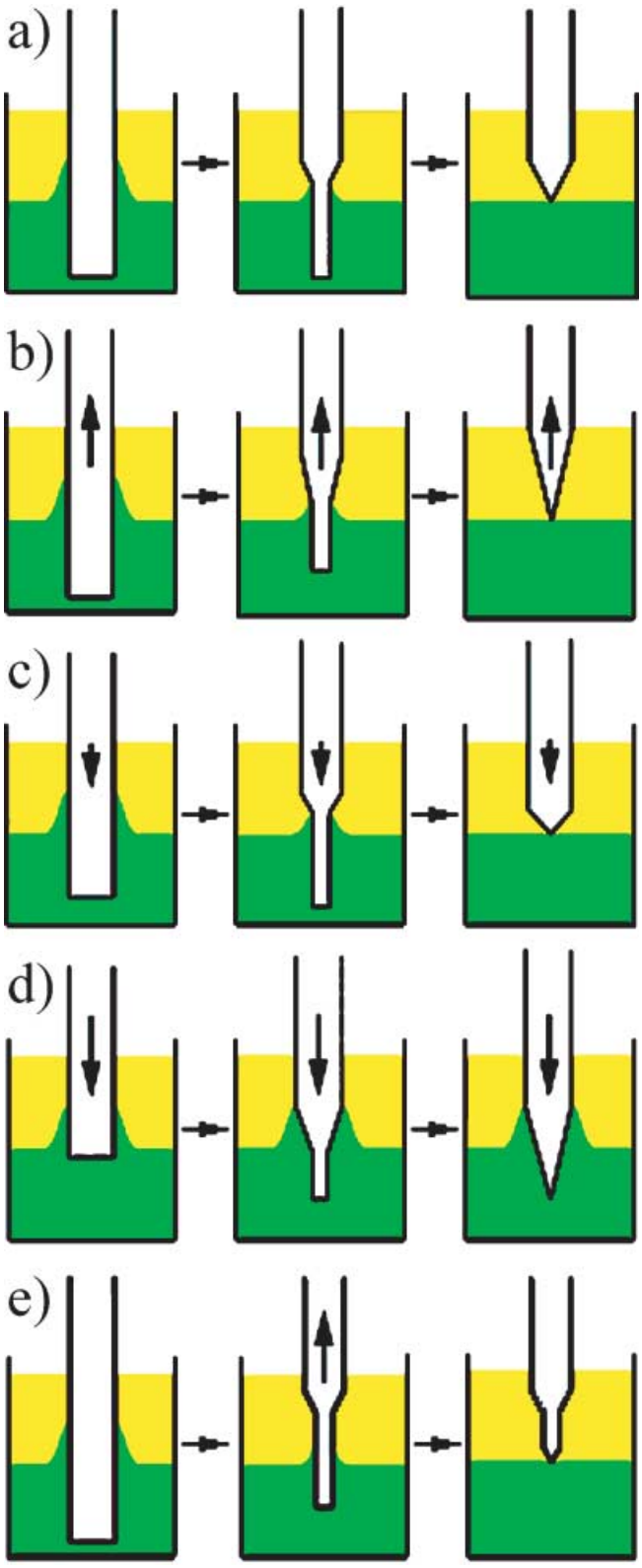

Fig. 3. Schematic diagrams of dynamic meniscus etching processes. All cases show the fibre at time zero (left), at time $\tau/2$ (middle) and at time τ (right). (a) Stationary tip. (b) Tip moving up (Case 1). (c) Tip moving down slowly (Case 2). (d) Tip moving down fast (Case 4). (e) Stepped tip for one step.

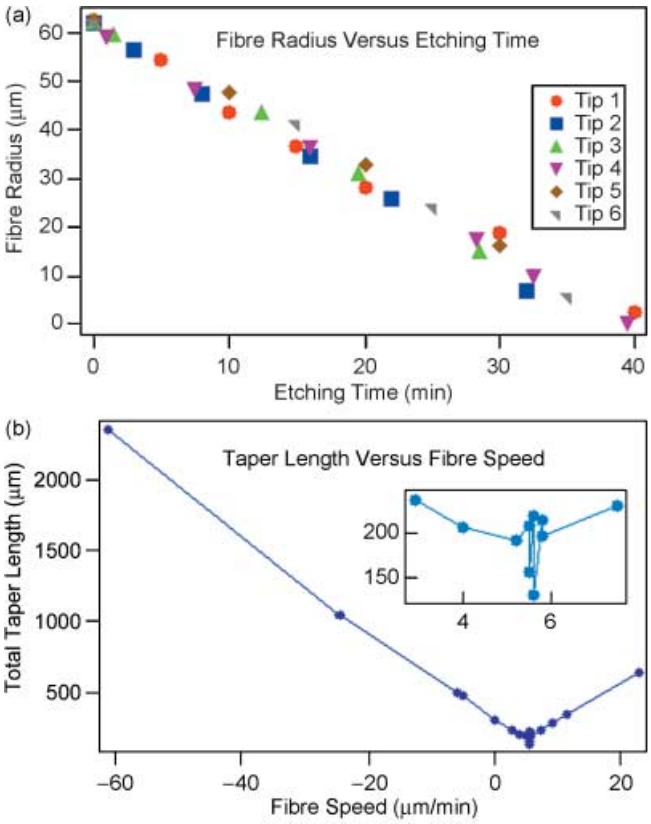

Fig. 4. (a) Fibre radius vs. etching time from stepped tip data. These data show a linear function, $r(t) = -1.55t + 61.0$ with an R^2 value of 0.992. For these fibres (diameter 125 ± 2 μm), $\tau = 39.4 \pm 1.3$ min. (b) Fibre speed vs. total taper length from constant speed Type 1 data. Inset: magnified region of Case 3 showing the non-linearity of the data.

made, with 3–6 different steps in each tip. The times and distances for each step were chosen to gain the greatest amount of information. The graph of fibre radius vs. etching time (Fig. 4a) shows a linear function. This result agrees with data from selective etching (Ohtsu, 1998). τ is defined here as the time required to etch a tip completely.

For the constant speed techniques, the fibre was moved in three different types of ways at constant speeds (Table 1). For Type 1, the fibre was moved for time ~τ then raised, resulting in a conical shape of variable cone angle and taper length (Fig. 5). For Type 2, the fibre was moved for time τ then left stationary for a variable time before being raised (Fig. 6). For Type 3, the fibre was moved for a time greater than τ. Types 2 and 3 produce more complicated tip shapes.

A simple model can be made to predict probe shapes fabricated with dynamic meniscus etching techniques. It is already known that the radius of the fibre linearly decreases with time when it is in contact with the acid and that the meniscus height naturally drops as the fibre radius decreases. The speed at which the meniscus drops is defined as h. The total taper length is defined as Y. The cone angle is simply equal to $2 \arctan[r(0)/Y]$, where $r(0)$ is the radius of the unetched

Table 1. Dynamic meniscus etching methods.

Stepped – Fibre is stationary then is raised quickly making a step. Multiple steps are possible per fibre.
Constant speed Type 1 – Fibre is moved for time τ. Case 1: speed < 0 μm min^{-1} Case 2: 0 < speed < 5.2 μm min^{-1} Case 3: 5.2 < speed < 5.8 μm min^{-1} Case 4: speed > 5.8 μm min^{-1}
Constant speed Type 2 – Fibre is moved down for time τ, then left stationary for a time t_2, allowing for meniscus relaxation to occur.
Constant speed Type 3 – Fibre is moved down for a time greater than τ, allowing for multiple tapers with increasing or decreasing cone angles.
Accelerating fibre motion – Fibre is moved at changing speeds resulting in gradual angle changes. Axially symmetric probes result.

fibre. Because the final result of stationary meniscus etching yields a conical shape, it can be assumed the meniscus speed is nearly constant during the majority of the etching process. Therefore $h\tau = Y$ for stationary meniscus etching. Stationary etching is of Type 1 at the limit of zero fibre speed, on the boundaries of Cases 1 and 2. To describe dynamic etching, two other variables are essential. We define x as the fibre speed and D as the term describing meniscus distortion resulting from the moving fibre. In general, D will depend on the fibre speed direction, interfacial surface tension and fibre geometry. Furthermore, the length that the meniscus is distorted can be assumed to vary linearly with fibre speed.

In the Type 1 constant speed method, four distinct cases arise that determine tip shape. Case 1 is when x is negative, i.e. the fibre is moving up. Here,

$$Y_1 = -(\tau - D_1)x + h\tau.$$

Case 2 is when x is positive, but sufficiently smaller than h. Because the fibre speed direction has changed, the distortion term is also expected to change. Therefore,

$$Y_2 = -(\tau - D_2)x + h\tau.$$

The natural meniscus speed will also depend on the fibre shape, and therefore it is expected that the initial meniscus speed is different than h, because the initial fibre shape is cylindrical rather than tapered. We will define the initial meniscus speed to be g. When the fibre speed is between h and g, small fluctuations of the meniscus can have large effects on its position and etching process. In addition, small deviations in the angle at which the fibre is positioned with respect to the etching solution will have large effects on the final probe shape. This represents Case 3, which is expected to have non-linear data and tips with small taper lengths that are difficult to predict and may have large angle changes. Finally, Case 4 is when the fibre is moving down faster than the meniscus is naturally dropping, causing the meniscus to be always above the taper at the cylinder of radius $r(0)$. A cone is made because different parts of the fibre are in contact with the acid for different lengths of time. At time τ, the lowest part of the taper is a sharp tip. Here,

$$Y_4 = (\tau - D_4)x + g\tau.$$

Because the fibre geometry is conical rather than tapered at the meniscus, the distortion term is expected to be slightly different from D_2. Finally, after the tip is made, it will still be submerged in the acid and will continue to etch, so the fibre has to be pulled up out of the acid. This shortens Y, but we will neglect this effect. Schematic diagrams of these cases are shown in Fig. 3.

To test this model, many probes were etched for a time of 44 min, where $t \sim \tau$. The data clearly show the four distinct cases that were predicted (Fig. 4b). Case 1, from the data with negative speeds, corresponds to the linear equation $Y_1 = -33.2x + 296$. Case 2, from data with positive speeds less than or equal to 5.2 μm min^{-1}, forms a line following $Y_2 = -21.6x + 298$. The data points of Case 4 with a speed greater than or equal to 5.8 μm min^{-1} form a line of the equation $Y_4 = 25.3x + 53.3$. Finally, Case 3, of speeds between 5.2 and 5.8 μm min^{-1}, is where the taper length is smallest but the data are non-linear. The boundary speeds of Case 3 may depend on step size and should always be between h and g. Probes made in the three linear Cases 1, 2 and 4 were all highly conical in shape whereas the probes made in Case 3 were sometimes very strangely shaped, with large angle changes in the taper.

These results agree well with the mathematical model. The values of h, g, D_1, D_2 and D_4 were calculated to be 7.5 ± 0.8 μm min^{-1}, 1.35 ± 0.09 μm min^{-1}, 6.1 ± 0.5 min, 17.8 ±

Fig. 5. Three Type 1 probes under low (left, scale bars = 10, 50 and 100 μm, respectively) and high (right, scale bars = 100 nm, 1 μm and 1 μm, respectively) magnification. Tip A was made going down at 5.4 μm min^{-1} for 44 min. Although made in the Case 3 region, the probe is very conical in shape with an angle of 33° and a total taper length of 207 μm. Tip B was made with the fibre stationary (0 μm min^{-1}) for 44 min. The cone angle is 21.2° and the total taper length is 288 μm. Tip C was made moving down at 57.3 μm min^{-1} for 44 min. The cone angle is 3° and the total taper length is 2350 μm.

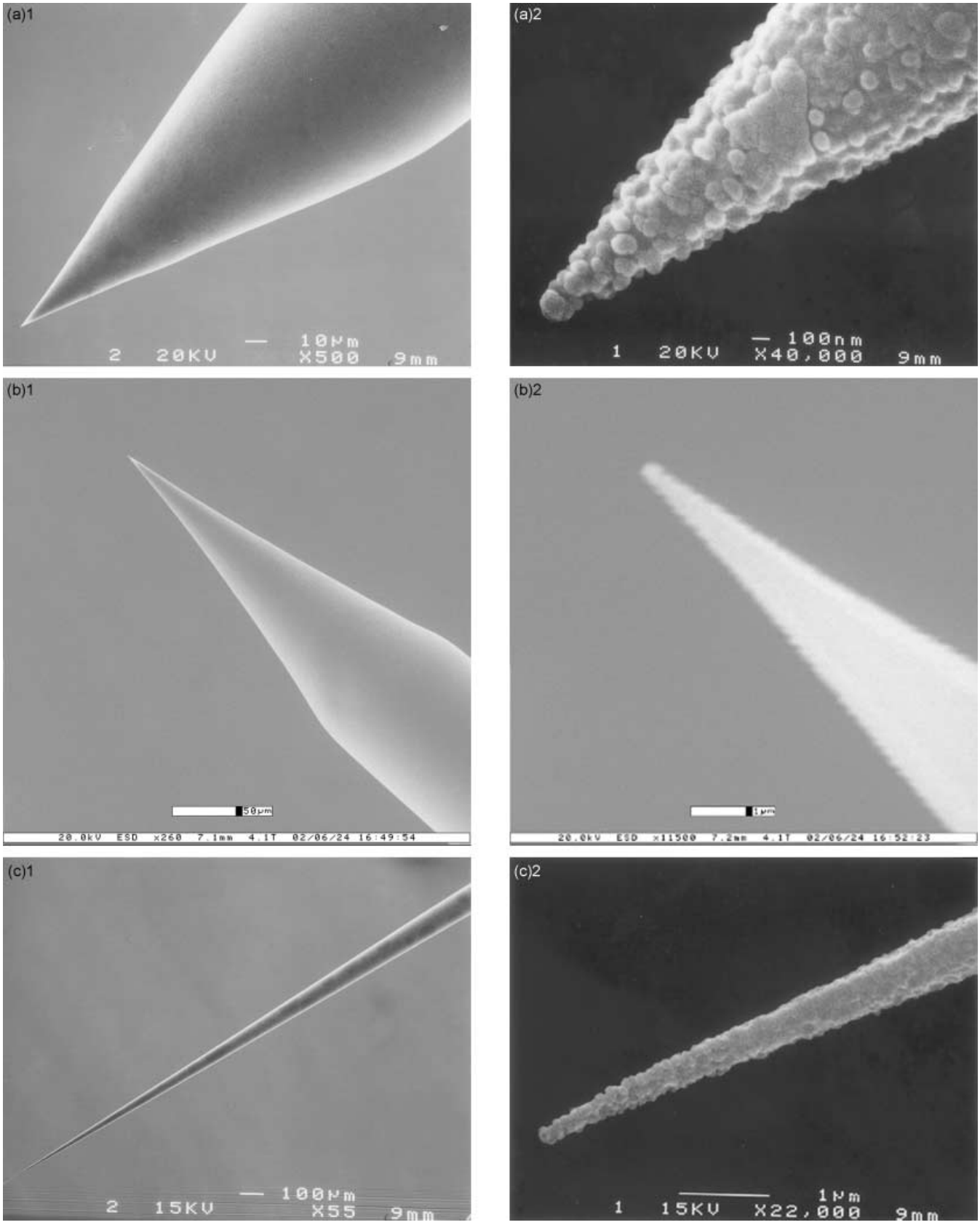
(a)1
2 20KV 10μm X500 9mm
(a)2
1 20KV 100nm X40,000 9mm
(b)1
50μm
20.0kV ESD x260 7.1mm 4.1T 02/06/24 16:49:54
(b)2
1μm
20.0kV ESD x11500 7.2mm 4.1T 02/06/24 16:52:23
(c)1
2 15KV 100μm X55 9mm
(c)2
1 15KV 1μm X22,000 9mm

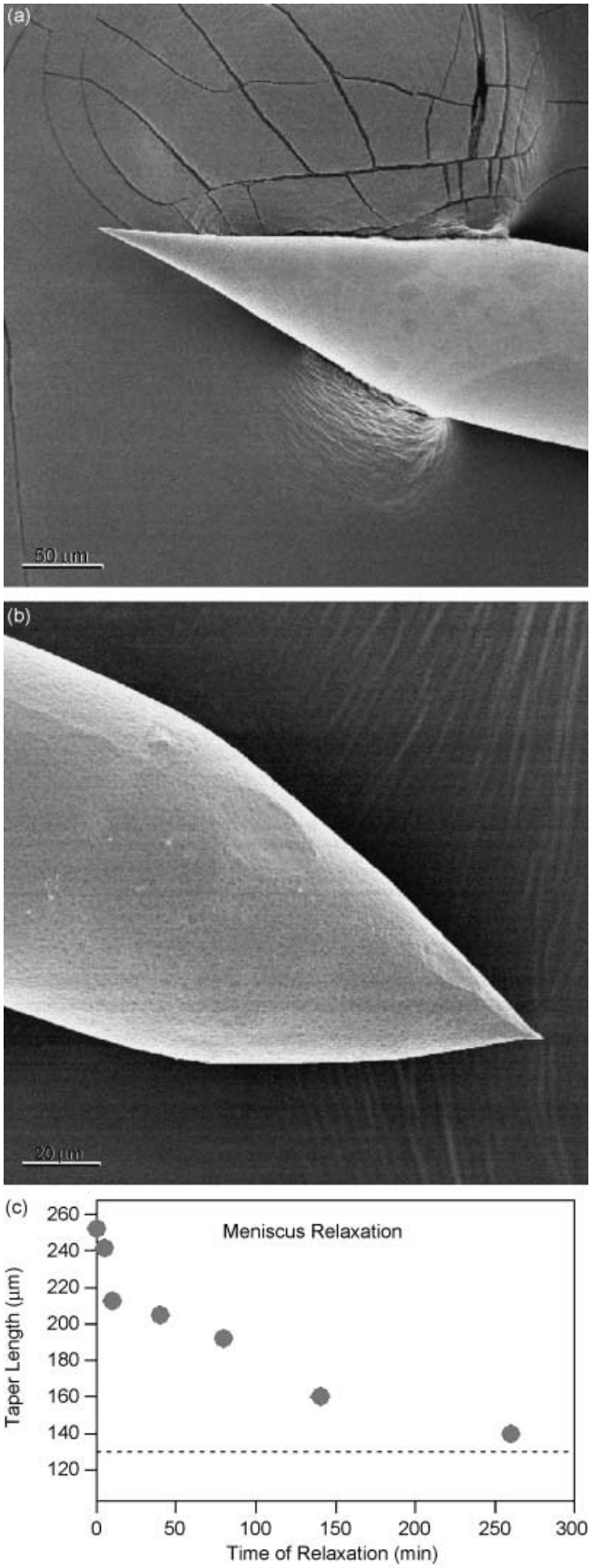

1.2 min and 14.1 ± 1.0 min, respectively. D_2 and D_4 are close in value because the meniscus distorts in the same direction, but they differ as a result of different fibre geometries. The large difference between D_1 and D_2 shows meniscus distortion is greater when the fibre is moving down. Because the probes were etched for a time of 44 min instead of exactly τ, the true values of h, g, D_2 and D_4 are expected to be slightly larger than those calculated from these data.

The constant speed Type 2 method lowers the fibre at a speed corresponding to Case 2 for time τ, then stops the fibre for an additional time t_2, allowing meniscus relaxation and further etching, and resulting in a shortened total taper length and a larger cone angle. A Type 2 method on a Case 1 or 4 speed would not have the desired effect of shortening Y because the meniscus distortion is in the opposite direction in Case 1 and the tip is under the meniscus in Case 4. Seven tips were etched using the Type 2 method, moving down at 4.58 µm min^{-1} for 40 min and then left stationary for 0–260 min before lifting up (Fig. 6). The graph of total taper length vs. relaxation time is asymptotically approaching the predicted taper length wherein the meniscus distortion is zero, in the form:

$$Y_R = (h - x)\tau + (D_2 x)\exp(-t_2/c),$$

where Y_R is the total taper length of the probe and c is a constant that depends on the original cone angle at $t_2 = 0$. This equation results from the assumption that the force which causes meniscus relaxation is proportional to the length of meniscus distortion, D_2x, thus setting up a damped harmonic oscillator solution with strong damping caused by meniscus surface tension and viscosity. The large experimental value of c shows that meniscus relaxation is very slow compared with meniscus distortion. In addition, the data for relaxation confirm that true values for h and D_2 are slightly larger than previously calculated.

The constant speed Type 3 method moves the fibre for a time greater than τ (Fig. 7a–c). If the tip is moving up for a time greater than τ, the result will be the same as in Type 1, Case 1, because after the tip is formed, any extra movement will simply lift the tip further away from the meniscus, causing no additional etching. This was confirmed experimentally. However, if the tip is moving down at a slow speed (Case 2) for a time greater than τ, the probe will form with an initial taper length, but as the fibre continues to move down into the acid, a second taper may be etched. If the conditions are right for this second taper to run to completion, and the fibre continues to

Fig. 6. Meniscus relaxation. (a,b) Tips A and B were both etched at 4.58 µm min^{-1} for 40 min, with a relaxation time, t_2, of 0 and 260 min, respectively. Scale bars = 50 and 20 µm, respectively. (c) Total taper length (µm) vs. relaxation time (min). The dotted line is the calculated total taper length value with no meniscus distortion. The data are best described by the equation, $Y = 130 + 112\exp(-t_2/109)$.

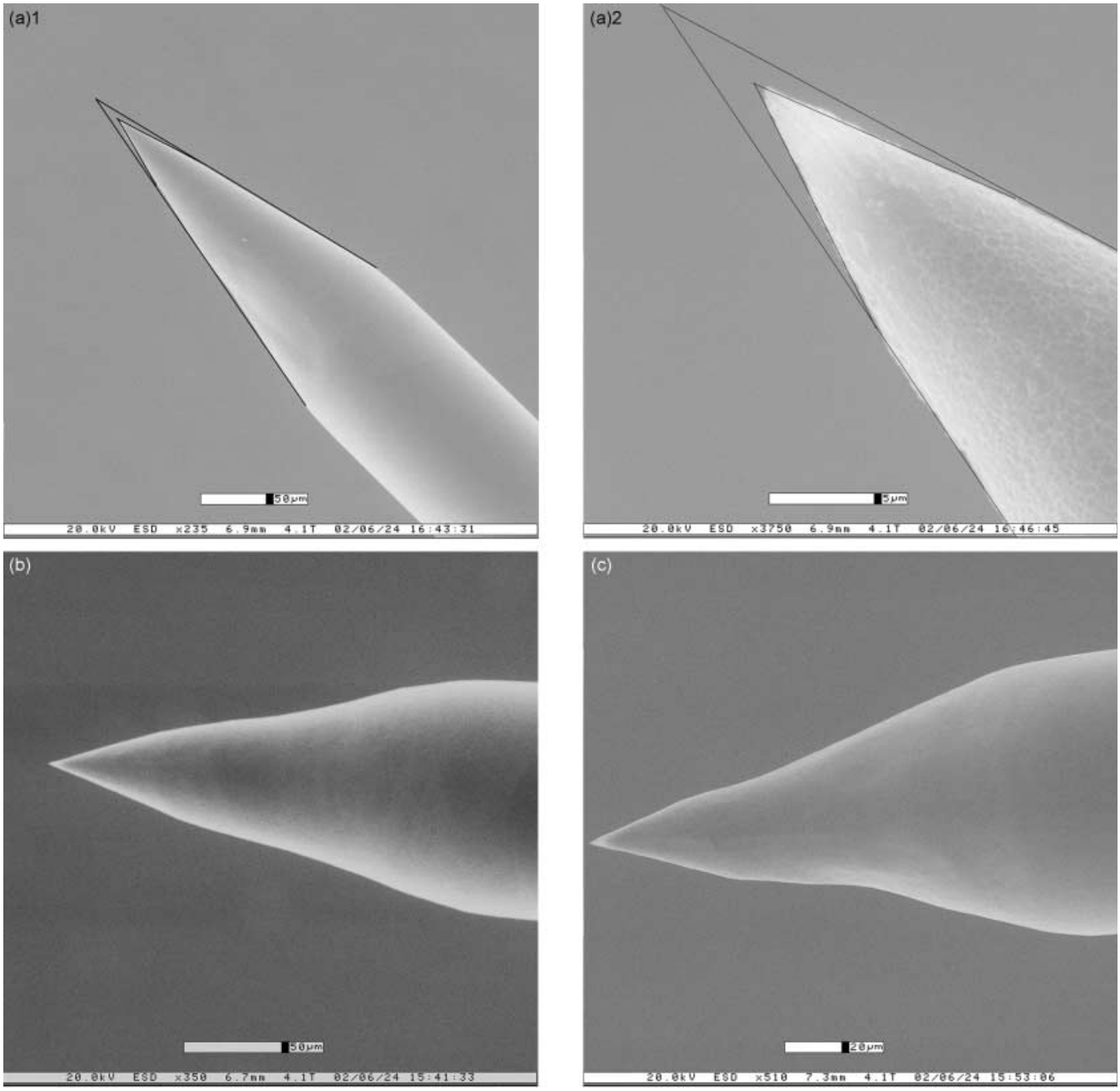

Fig. 7. Tips A, B and C are Type 2. Tip A was etched at 1.15 μm min^{-1} going down for 115 min. The whole probe is shown on the left (scale bar = 50 μm) with the first and second tapers outlined having cone angles of 25.4° and 28.7°, respectively. The high magnification (scale bar = 5 μm) of Tip A reveals a third taper of angle 39.2° outlined on the right. Tips B and C were etched at 4.58 μm min^{-1} for 70 and 115 min, respectively (scale bars = 50 and 20 μm, respectively). The second taper has an increasing angle change but the third taper (in progress) has a decreasing angle change. In Tip C, the third taper has progressed further. In Tips D and E, the accelerating fibre motion technique was used. Tip D was etched for 40 min with the fibre speed linearly changing from –0.122 μm min^{-1} to –9.79 μm min^{-1} (scale bars = 100 and 1 μm, respectively). The initial cone angle, at the beginning of the taper, is ~20.2° but the cone angle at the tip is ~11°. Tip E was etched for 44 min with the fibre speed linearly changing from –24.48 μm min^{-1} to 22.92 μm min^{-1} (scale bars = 100 μm and 100 nm, respectively). The initial cone angle is ~14.1° and the tip cone angle is ~39.8°.

move down, subsequent tapers can be etched. Multiple tapers can either increase or decrease the tip angle depending on the relation between fibre speed, meniscus speed and meniscus distortion. The meniscus speed will change as the probe geometry changes for the second or subsequent tapers. If the fibre is moving down slower than the meniscus speed of the subsequent taper, the cone angle will increase relative to the previous cone angle and the total taper length of the probe will

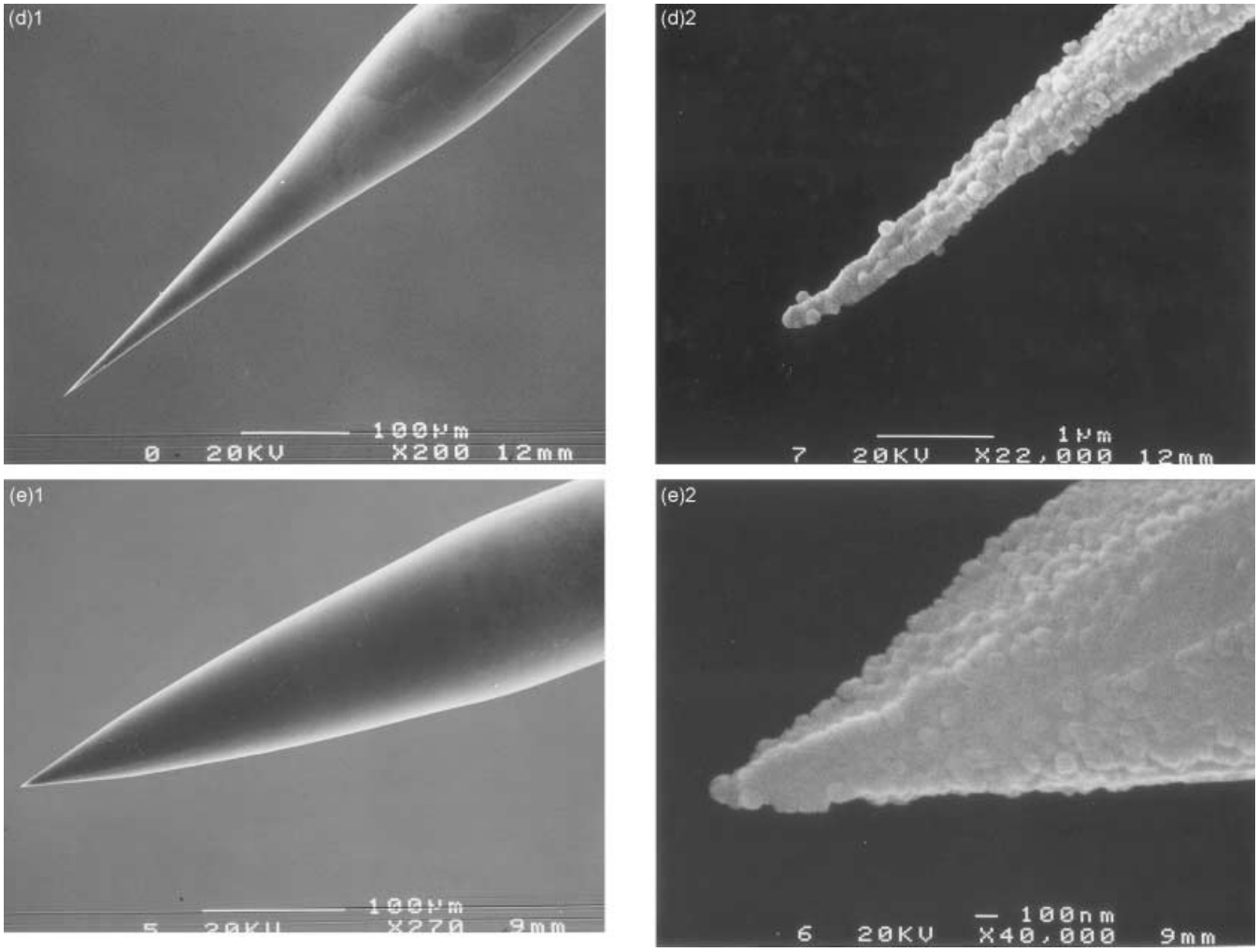

Fig. 7. continued.

decrease. If the speed of the fibre is faster than the speed of the meniscus for the subsequent taper, the meniscus will start to move to the top of the cone, etching away the fibre as it moves and resulting in a decreasing angle change. Using this technique, many complicated probe shapes have been made, though more research is needed to characterize this method fully.

In the accelerating fibre motion technique, the fibre speed is changed as the etching is taking place, resulting in probe shapes with slowly changing angles (Fig. 7d, e). The speed can be changed in any possible way, creating a large variety of shapes. Although this technique has not been studied in detail yet, the initial results are very promising. When the fibre is pulled up at a linearly increasing speed, the cone angle starts larger and ends smaller at the tip. When the fibre speed increases linearly, the result is a tip with a smaller angle at the top of the taper and a larger angle at the tip. There have been studies suggesting that a compound parabolic concentrator probe, or CPC, will have the highest throughput of any shape (Paesler & Moyer, 1996). The changing speed dynamic meniscus etching technique may prove to be the easiest way to make such parabolic type probes. In addition, many other axially symmetric geometries can be made in this way, though much experimentation must be carried out in order to characterize and predict this technique. In particular, the meniscus speed, distortion and relaxation must be studied as a function of cone angle.

Conclusions

Dynamic meniscus etching has been shown to be an easy method for the production of a variety of probe shapes for NSOM. By analysing stepped probes, the etching process was shown to decrease the fibre radius linearly as a function of time. A model was formulated to determine the probe shape that depends on the fibre speed, the meniscus speed and the distortion of the meniscus for the constant speed method etched for a time τ. This model agrees with the data collected for constant speed tips etched for 44 min. Another constant speed method relies on meniscus relaxation to shorten the

taper length. Multiple tapered tips made by a constant speed method for a time greater than τ were also explained and studied, showing evidence of two different types of multiple etches in which angle changes are either positive or negative. The accelerating fibre motion technique was also studied, and this results in tips with gradual angle changes. By controlling the probe shape and cone angle, resolution and throughput can be optimized for a particular NSOM application.

Acknowledgements

The work was supported by the Experimental Physical Chemistry Division of the National Science Foundation. The authors thank Ron Wilson and Gordon Vrdoljak for their SEM expertise, and Lynn Lee and Kelly Knutsen for their valuable help and discussions.

References

Chuang, Y.H., Sun, K.G., Wang, C.J., Huang, J.Y. & Pan, C.L. (1998) A simple chemical etching technique for reproducible fabrication of robust scanning near-field fibre probes. *Rev. Sci. Instrum*. **69**, 437–439.

Dunn, R.C. (1999) Near-field scanning optical microscopy. *Chem. Rev*. **99**, 2891–2927.

Held, T., Emonin, S., Marti, O. & Hollricher, O. (2000) Method to produce high-resolution scanning near-field optical microscope probes by beveling optical fibres. *Rev. Sci. Instrum*. **71**, 3118–3122.

Hoffmann, P., Duoit, B. & Salathe, R. (1995) Comparison of mechanically drawn and protection layer chemically etched optical fibre tips. *Ultramicroscopy*, **61**, 165–170.

Islam, M.N., Zhao, X.K., Said, A.A., Mickel, S.S. & Vail, C.F. (1997) High-efficiency and high-resolution fibre-optic probes for near-field imaging and spectroscopy. *Appl. Phys. Lett*. **20**, 2886–2888.

Jia-Lin, S., Juan-Hua, X., Guang-Yan, T., Ji-Hua, G., Jun, Z., Ai-Fang, X. & Ze-Bo, Z. (2001) Fabrication and application of near-field optical fibre probe. *Chin. Phys. Soc*. **10**, 631–635.

Krogmeier, J.R. & Dunn, R.C. (2001) Focused ion beam modification of atomic force microscopy tips for near-field scanning optical microscopy. *Appl. Phys. Lett*. **79**, 4494–4496.

Lambelet, P., Sayah, A., Pfeffer, M., Philipona, C. & Marquis-Weible, F. (1998) Chemically etched fibre tips for near-field optical microscopy: a process for smoother tips. *Appl. Opt*. **37**, 7289–7292.

Liu, X., Wang, J. & Li, D. (1998) Simple device and reproducible approach for producing high efficiency optical fibre tips for a scanning optical microscope. *Rev. Sci. Instrum*. **69**, 3439–3440.

Muramatsu, H., Homma, K., Chiba, N., Yamamoto, N. & Egawa, A. (1999) Dynamic etching method for fabricating a variety of tip shapes in the optical fibre probe of a scanning near-field microscope. *J. Microsc*. **194**, 383–387.

Ohtsu, M. (1998) *Near-Field Nano/Atom Optics and Technology*. Springer-Verlag, Tokyo.

Paesler, M.A. & Moyer, P.J. (1996) *Near-Field Optics: Theory, Instrumentation, and Applications*. Wiley, New York.

Sayah, A., Philipona, C., Lambelet, P., Pfeffer, M. & Marquis-Weible, F. (1998) Fibre tips for scanning near-field optical microscopy fabricated by normal and reverse etching. *Ultramicroscopy*, **71**, 59–63.

Spajer, M., Parent, G., Bainer, C. & Charraut, D. (2000) Shaping the reflection near-field optical probe: finite domain time difference modelling and fabrication using a focused ion beam. *J. Microsc*. **202**, 45–49.

Stöckle, R., Fokas, C., Deckert, V. & Zenobi, R. (1999) High-quality near-field optical probes by tube etching. *Appl. Phys. Lett*. **75**, 160–162.

Unger, M.A., Kossakovski, D.A., Kongovi, R., Beauchamp, J.L., Baldeschwieler, J.D. & Palanker, D.V. (1998) Etched chalcogenide fibres for near-field infrared scanning microscopy. *Rev. Sci. Instrum*. **69**, 2988–2993.

Valaskovic, G.A., Holton, M. & Morrison, G.H. (1995) Parameter control, characterization, and optimization in the fabrication of optical fibre near-field probes. *Appl. Opt*. **34**, 1215–1228.